

Vehicle positioning in urban environments using particle filtering-based global positioning system, odometry, and map data fusion

Abdelkabar Lahrech¹, Aziz Soulhi²

¹MRI Laboratory, Faculté Polydisciplinaire, Khouribga, Sultan Moulay Slimane University, Beni Mellal, Morocco

²Superior National School of Mines, Rabat, Morocco

Article Info

Article history:

Received Aug 17, 2022

Revised Sep 27, 2022

Accepted Oct 13, 2022

Keywords:

Digital maps
Global positioning system navigation
Multi-sensor fusion
Non-linear filtering
Particle filter

ABSTRACT

This article presents a new method for land vehicle navigation using global positioning system (GPS), dead reckoning sensor (DR), and digital road map information, particularly in urban environments where GPS failures can occur. The odometer sensors and map measure can be used to provide continuous navigation and correct the vehicle location in the presence of GPS masking. To solve this estimation problem for vehicle navigation, we propose to use particle filtering for GPS/odometer/map integration. The particle filter is a method based on the Bayesian estimation technique and the Monte Carlo method, which deals with non-linear models and is not limited to Gaussian statistics. When the GPS sensor cannot provide a location due to the number of satellites in view, the filter fuses the limited GPS pseudo-range data to enhance the vehicle positioning. The developed filter is then tested in a transportation network scenario in the presence of GPS failures, which shows the advantages of the proposed approach for vehicle location compared to the extended Kalman filter.

This is an open access article under the [CC BY-SA](#) license.



Corresponding Author:

Abdelkabar Lahrech

MRI Laboratory, Faculté Polydisciplinaire, Khouribga, Sultan Moulay Slimane University

Beni Mellal, Morocco

Email: a.lahrech@usms.ma

1. INTRODUCTION

Over the past three decades, the use of positioning and navigation technologies has shown a remarkable increase in several areas, particularly in transportation applications. Classically, the global positioning system (GPS) is a key sensor for many navigation systems. However, in some dense urban environments, GPS positioning might not be accurate or even unavailable due to multi-path problems or poor satellite visibility. On the other hand, the signal may be also reflected or blocked by high-rise buildings in deeper urban canyons which is more challenging for GPS positioning [1]. Therefore, different types of sensors have been used to aid vehicle's positioning in the urban environment, for example, dead-reckoning (DR) sensors such as odometers can be used to provide a continuous navigation [1]–[3], which considered as a wheel speed sensor. This sensor is a wheel encoder device that generates digital pulses for each revolution of the wheel and allows an estimation of the distance traveled by the vehicle in a period of time. Moreover, in most transportation applications, the vehicle moves along a road network and a digital road map can be also used to correct the estimated position. In order to improve the positioning of the vehicle, the best correspondence between its location and one of the roads of the digital map must be realized, this

procedure is called map-matching. Many methods have been developed for solving the map-matching problem [4]–[6].

The aim here is to propose a map-aided positioning GPS-based system that provides an accurate and continuous location of the vehicle. In this case, one has a network representation of the map. It consists of a set of 2-D curves, called arcs, each of them being linked by points (nodes) which are also used as measures. There are several various principles to match the estimated location with an arc in the map. The most commonly used method is based on a purely geometric technique [7] such as point-to-point matching, point-to-arc matching, and curve-to-curve matching. These methods are based on a distance criterion but are highly susceptible to positioning and mapping errors, especially when considering maps in areas with a dense road network [8]–[11].

The extended Kalman filter (EKF) [12], [13] is commonly used to integrate the GPS data, odometer, and map measurements. However, due to the linearization step of the non-linear model in the EKF, it will introduce large estimation errors over time. The Kalman filter and EKF filter assume that the measurement noise can be described using a Gaussian density function. However, this assumption is not valid in the presence of nonlinear models and measurement noise, not Gaussian. Therefore, several approaches have been developed to improve the accuracy and efficiency of this filter for applications with non-Gaussian densities of the states, and/or measurement noise. These modifications include fuzzy correntropy filter CKF with adaptive kernel size for optimization [14] and Kalman-filter-based sine-cosine algorithm (KFSCA) [15]. These algorithms are inspired by the Kalman filter. The main difference is that these methods use a cost function to be minimized instead of computing the conventional Kalman gain.

During the last decades, new filtering techniques have been developed for mobile navigation like (unscented Kalman filter (UKF) [16], [17] and sequential Monte-Carlo methods [18], [19]). These methods can account for nonlinear models and non-Gaussian statistics without a linearization stage, like the EKF. Some works are developed in this case for mobile navigation. One can, for example, cite the GPS and inertial navigation system (INS) integration [20], the GPS/inertial measurement unit (IMU)/light detection and ranging (LIDAR) sensor integration [21], and IMU/anti-lock braking system (ABS)/map fusion [22].

This work details, a centralized fusion algorithm for land vehicle navigation in urban areas with a partial or total GPS outage. In case of a partial GPS outage, which is often the case in urban environments, our method proposes to use the available pseudo-range data, even if they are not enough to obtain a GPS position. In case of a total GPS outage, the filter uses also dead-reckoning sensors (differential odometry) and a road map database to provide continuous localization. This multi-sensor fusion problem is solved by particle filtering [23], [24] that fuses the measurements of each sensor and sequentially integrates them to estimate the 3-D localization of the vehicle.

2. VEHICLE SYSTEM AND SENSOR MEASUREMENT MODELING

The multi-sensor estimation problem can be modeled by the state vector detailed below. The vehicle model used for fusion is presented first; secondly, the measurement model which include the respectively the GPS, partial GPS measurements (computed with limited GPS pseudo-range data), odometer and data map information are stated. Finally, various fusion strategies are then presented for urban navigation in order to improve the proposed filter performance.

2.1. Vehicle dynamics modeling

Consider a vehicle whose state vector consists of its position, velocity, and acceleration in the east-north-up (ENU) frame. They are presented along the x , y , and z -coordinates at time k by (1).

$$X_k = (\gamma_k^x, v_k^x, x_k, \gamma_k^y, v_k^y, y_k, \gamma_k^z, v_k^z, z_k)^T \quad (1)$$

From this consideration, the relation between consecutive states can be written, along the x -component, for instance:

$$\begin{cases} \gamma_k^x &= \gamma_{k-1}^x + w_k^{\gamma^x} \\ v_k^x &= \gamma_{k-1}^x \Delta k + v_{k-1}^x + w_k^{v^x} \\ x_k &= x_{k-1} + v_{k-1}^x \Delta k + w_k^{x^x} \end{cases}$$

where $(w_k^{\gamma^x}, w_k^{v^x}, w_k^x)$ are unknown independent zero-mean Gaussian process noise and Δk defines the sampling time.

This system of equation can be written in the matrix format, as:

$$\begin{pmatrix} \gamma_k^x \\ v_k^x \\ x_k \end{pmatrix} = \begin{pmatrix} 1 & 0 & 0 \\ \Delta k & 1 & 0 \\ 0 & \Delta k & 1 \end{pmatrix} \begin{pmatrix} \gamma_{k-1}^x \\ v_{k-1}^x \\ x_{k-1} \end{pmatrix} + \begin{pmatrix} w_k^{\gamma^x} \\ w_k^{v^x} \\ w_k^x \end{pmatrix}$$

So, the dynamics model, for all components becomes as (2).

$$X_k = FX_{k-1} + W_k \quad (2)$$

where F is the linear dynamics matrix of the system and W_k is the Gaussian process noise with $W_k \sim \mathcal{N}(0, Q_k)$ due to the model and Q_k covariance matrix.

$$F = \begin{pmatrix} F_x & \mathbf{0}_{3 \times 3} & \mathbf{0}_{3 \times 3} \\ \mathbf{0}_{3 \times 3} & F_y & \mathbf{0}_{3 \times 3} \\ \mathbf{0}_{3 \times 3} & \mathbf{0}_{3 \times 3} & F_z \end{pmatrix} \quad F_u = \begin{pmatrix} 1 & 0 & 0 \\ \Delta k & 1 & 0 \\ 0 & \Delta k & 1 \end{pmatrix}$$

Δk represents the sampling period, $\mathbf{0}_{3 \times 3}$ is a null matrix of 3 rows and 3 columns and $F_x = F_y = F_z$.

2.2. Measurement model

There are four measurement models. The first is the GPS data without outages. The second is the GPS data with partial outages. The last two models differential odometry, and a road map database. The details of each model are explained below.

2.2.1. GPS data without outages

GPS data without outages: The GPS observation obtained from the ProPak-G2 NovaAtel receiver is computed in the WGS84 system and is converted via a projection in the local coordinates system (East, North, up). The observation equation of GPS positions is expressed as:

$$\mathcal{Z}_k^{\text{GPS}} = \begin{pmatrix} x_k^{\text{GPS}} \\ y_k^{\text{GPS}} \\ z_k^{\text{GPS}} \end{pmatrix} = h^{\text{GPS}}(X_k) + V_k^{\text{GPS}}$$

where h^{GPS} is the evolution function of the GPS measurements and V_k^{GPS} is a Gaussian white noise R_k^{GPS} .

2.2.2. GPS data with partial outage

When the available satellite signals are not sufficient for computing a GPS position (less than 4), the filter uses the limited GPS pseudo-range measurements to improve the vehicle location, since they contain the positioning information. For instance, with three satellites, The pseudo-range ρ_k^j for the j th satellite can be written as (3).

$$\begin{cases} \rho_k^j &= \sqrt{(x_k^j - x_k)^2 + (y_k^j - y_k)^2 + (z_k^j - z_k)^2} + c\delta t, \\ j &= \{1, \dots, 3\}. \end{cases} \quad (3)$$

where c is the speed of light and (x_k^j, y_k^j, z_k^j) are the coordinates of the j th satellite $j = \{1, \dots, 3\}$. (x_k, y_k, z_k) and δt denotes the receiver position in three dimensions and its clock offset from the system time respectively.

To compute the partial GPS measures $\mathcal{Z}_k^{\text{PGPS}}$, the predicted location parameters of the state vector by the proposed filter and the non-linear least squares method has been used for solving the GPS navigation solution. The $\mathcal{Z}_k^{\text{PGPS}}$ measures are computed in the Cartesian coordinates system (ECEF) and are converted via a projection in the local coordinates system (UTM). We have:

$$\mathcal{Z}_k^{\text{PGPS}} = h^{\text{PGPS}}(X_k) + V_k^{\text{PGPS}}$$

where h^{PGPS} is the evolution function of the PGPS measurements and V_k^{PGPS} is a Gaussian white noise of mean null and covariance R_k^{PGPS} .

2.2.3. Differential odometry

If the GPS sensor cannot provide any vehicle positions, the differential odometry sensor [25]) is used. It delivers a quantified measurement Z_k^{ODO} of the left and right wheels' elementary displacements and the heading angle of the vehicle [26] as shown in Figure 1:

$$Z_k^{ODO} = \begin{pmatrix} \Delta D_k^R \\ \Delta D_k^L \\ \theta_k^{ODO} \end{pmatrix} = h^{ODO}(X_k) + V_k^{ODO} \tag{4}$$

where $(\Delta D_k^R, \Delta D_k^L)$ indicates the right and left wheel elementary displacements, θ_k^{ODO} is the orientation of the vehicle measured with respect to the horizontal axis, h^{ODO} is the evolution function of odometer measurements and V_k^{ODO} is a Gaussian white noise of mean null and covariance matrix R_k^{ODO} , i.e.,

$$\begin{cases} \Delta D_k^R = \frac{\sqrt{(\Delta D_k^{R,x})^2 + (\Delta D_k^{R,y})^2}}{r_R} + V_k^{ODO,R} \\ \Delta D_k^L = \frac{\sqrt{(\Delta D_k^{L,x})^2 + (\Delta D_k^{L,y})^2}}{r_L} + V_k^{ODO,L} \\ \theta_k^{ODO} = \arctan\left(\frac{v_k^y}{v_k^x}\right) + V_k^{ODO,\theta} \end{cases}$$

where r_L is the radius of the left wheel and r_R is the radius of the right wheels, respectively, and $(\Delta D_k^{L,x}, \Delta D_k^{L,y})$ and $(\Delta D_k^{R,x}, \Delta D_k^{R,y})$ are the vehicle right and left displacement respectively along x and y components for the wheel. These displacements are expressed for both wheels according to the state vector.

$$\begin{cases} \Delta D_k^{R,x} = v_{k-1}^x \Delta k + \frac{e}{2} \left(\frac{v_k^y}{\|v_k\|} - \frac{v_{k-1}^y}{\|v_{k-1}\|} \right) \\ \Delta D_k^{R,y} = v_{k-1}^y \Delta k - \frac{e}{2} \left(\frac{v_k^x}{\|v_k\|} - \frac{v_{k-1}^x}{\|v_{k-1}\|} \right) \\ \Delta D_k^{L,x} = v_{k-1}^x \Delta k - \frac{e}{2} \left(\frac{v_k^y}{\|v_k\|} - \frac{v_{k-1}^y}{\|v_{k-1}\|} \right) \\ \Delta D_k^{L,y} = v_{k-1}^y \Delta k + \frac{e}{2} \left(\frac{v_k^x}{\|v_k\|} - \frac{v_{k-1}^x}{\|v_{k-1}\|} \right) \end{cases}$$

where e is the distance between the left and right rear wheels.

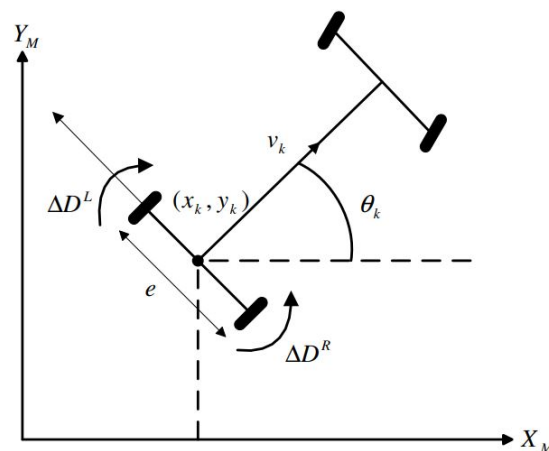


Figure 1. Differential odometry model

2.2.4. Road map database

When the GPS positioning is not available, the estimator also exploits the map measurements. The map database is composed of a large set of roads and each road consists of a number of segments. Hence, a segment is described by a finite set of nodes, among which a node represents a start/final node from one segment to another in the map. Here, the node coordinates are the position information $(x_k^{\text{MAP}}, y_k^{\text{MAP}})$ and the orientation θ_k^{MAP} of the road segment [27].

$$\mathcal{Z}_k^{\text{MAP}} = \begin{pmatrix} x_k^{\text{MAP}} \\ y_k^{\text{MAP}} \\ \theta_k^{\text{MAP}} \end{pmatrix} = h^{\text{MAP}}(X_k) + V_k^{\text{MAP}} \quad (5)$$

where h^{MAP} is the evolution function of map measurements and V_k^{MAP} is a Gaussian white noise of mean null and covariance matrix R_k^{MAP} .

$$\begin{cases} x_k^{\text{MAP}} &= x_k + V_k^{\text{MAP},x} \\ y_k^{\text{MAP}} &= y_k + V_k^{\text{MAP},y} \\ \theta_k^{\text{MAP}} &= \arctan\left(\frac{v_k^y}{v_k^x}\right) + V_k^{\text{MAP},\theta} \end{cases} \quad (6)$$

3. VEHICLE TRAJECTORY ESTIMATION USING PARTICLE FILTERING

We develop here a method based on particle filtering for localization vehicles in urban areas, with GPS outages. This method allows estimating the vehicle's dynamics parameters by fusing GPS, PGPS, odometer measures, and road map data. It can be summarized into five points, which are initialization, the evolution of particles, weighting, estimation, and resampling.

3.1. Initialization

In this step, each particle $\{X_0^i\}_{i=\{1,\dots,N\}}$ must be first initialized by a set of random state samples using the initial density $P(X_0)$ which represents the initial available information. The weights assigned to each particle, $\{w_0^i\}_{i=\{1,\dots,N\}}$, are taken equal to $\frac{1}{N}$, where N is the number of particles. These weights determine the importance of each particle in the estimation process.

3.1.1. Evolution of particles

The particles $\{X_{k-1}^i\}_{i=\{1,\dots,N\}}$ of the state space evolve according to the dynamics model (7), through the generation of N independent noise realizations W_k^i with law $P(W_k)$. For each particle, the algorithm uses this equation to compute an estimate of the future state. The evolution step is then used in the weighting step, where new sensors measurements is integrated to refine the estimation of the state of the vehicle.

$$X_k^i = F X_{k-1}^i + W_k^i \quad (7)$$

3.2. Weighting

The weights w_k^i can then be updated by the measures available at time k according to Bayes' rule as in (8).

$$w_k^i = \frac{P(\mathcal{Z}_k | X_k^i)}{\sum_{j=1}^N P(\mathcal{Z}_k | X_k^j)} w_{k-1}^i \quad (8)$$

This step computes the weight of each particle using the available observation \mathcal{Z}_k at time k . So, three main cases, which are the available GPS measures, the partial GPS outage, and the total GPS outage, can be developed.

a. GPS measures are available

In this case, the estimator uses only the GPS measure ($\mathcal{Z}_k = \mathcal{Z}_k^{\text{GPS}}$) to estimate the parameters (acceleration, velocity, and position) of the vehicle. Note that a GPS solution is considered available when pseudo-range measurements are greater than or equal to 4.

$$P(\mathcal{Z}_k | X_k^i) = P(\mathcal{Z}_k^{\text{GPS}} | X_k^i) \quad (9)$$

The log-likelihood function $V(\mathcal{Z}_k | X_k^i)$ is then proportional to:

$$\begin{aligned} V(\mathcal{Z}_k | X_k^i) &\sim \ln(P(\mathcal{Z}_k^{\text{GPS}} | X_k^i)) \\ &\sim \|\mathcal{Z}_k^{\text{GPS}} - H^{\text{GPS}} X_k^i\|_{R^{\text{GPS}}}^2 \end{aligned}$$

where $\|\cdot\|_R^2$ is equal to $(\cdot)^T R^{-1}(\cdot)$. Then, we normalized the weights of the particles as (10).

$$w_k^i = \frac{w_k^i}{\sum_{j=1}^N w_k^j} \quad (10)$$

b. Partial GPS outage

The proposed approach exploits the available GPS pseudo-range measures even if it is less than 4 because they contain positioning information. For this purpose, one develops partial measures of the GPS sensor from the available pseudo-range measures. The filter uses the predicted parameters of the state vector and the least squares method to compute a partial GPS measure. For instance, with three satellites in view, the pseudo-range ρ_k^j for the j th satellite can be written as (11).

$$\rho_k^j = \sqrt{(x_k^j - x_k)^2 + (y_k^j - y_k)^2 + (z_k^j - \hat{z}_{k/k-1})^2} + c\delta t \quad (11)$$

where $j = \{1, \dots, 3\}$ and $\hat{z}_{k/k-1}$ is the filter-based prediction of z_k , i.e., $\hat{z}_{k/k-1} = \sum_{i=1}^N w_{k-1}^i z_k^i$.

To compute the receiver position, the predicted location $\hat{z}_{k/k-1}$ of particle filter and the least squares method can be used if three pseudorange measures were available. With two satellites in view, the method requires two components of the predicted state vector $\hat{y}_{k/k-1}$ and $\hat{z}_{k/k-1}$ for solving the GPS navigation.

During partial GPS outages, the filter also fuses the odometer measures and digital road map to estimate the displacement. The problem fundamental now is to correlate the previous predicted state and associate it with the map data information. For this purpose, it is fundamental to match the predicted location of the vehicle with the road network on the map. There are several solutions to this multi-sensor tracking problem, such as a probabilistic approach or multi-hypothesis navigation system [28], map likelihood calculation [29]. Other algorithms use the statistical approach, deterministic model approaches, fuzzy logic, and belief theory [30]. The chosen solution is the probabilistic approach using the Mahalanobis distance as coherence metric [31], [32]. This metric is computed between the 2-D predicted map position

$\hat{\mathcal{Z}}_{k|k}^{\text{MAP}} = \sum_{i=1}^N \omega_k^{(i)} h^{\text{MAP}}(X_{k|k}^i)$ and each map attribute (2-D location of the nodes and segment direction), $\mathcal{Z}_m^{\text{MAP}}$, $m = \{1, \dots, m_{\text{max}}\}$

We calculate the Mahalanobis distance $d_m = (\mathcal{Z}_m^{\text{MAP}}, \hat{\mathcal{Z}}_{k|k}^{\text{MAP}})$ using two directions of the road:

$$d_{1,m} = \min_m \left[(\mathcal{Z}_m^{\text{MAP}1} - \hat{\mathcal{Z}}_{k|k}^{\text{MAP}})^T (\tilde{P}_{k|k}^{\text{MAP}})^{-1} (\mathcal{Z}_m^{\text{MAP}1} - \hat{\mathcal{Z}}_{k|k}^{\text{MAP}}) \right] \quad (12)$$

$$d_{2,m} = \min_m \left[(\mathcal{Z}_m^{\text{MAP}2} - \hat{\mathcal{Z}}_{k|k}^{\text{MAP}})^T (\tilde{P}_{k|k}^{\text{MAP}})^{-1} (\mathcal{Z}_m^{\text{MAP}2} - \hat{\mathcal{Z}}_{k|k}^{\text{MAP}}) \right] \quad (13)$$

where

$$\begin{aligned} \mathcal{Z}_m^{\text{MAP}1} &= (x_m^{\text{MAP}}, y_m^{\text{MAP}}, \theta_m^{\text{MAP}}); \\ \mathcal{Z}_m^{\text{MAP}2} &= (x_m^{\text{MAP}}, y_m^{\text{MAP}}, \theta_m^{\text{MAP}} + \pi); \end{aligned} \quad (14)$$

$\tilde{P}_{k/k}^{\text{MAP}}$ indicates the error covariance of the predicted map measure. It is computed as:

$$\tilde{P}_{k/k}^{\text{MAP}} = \sum_{i=1}^N \omega_k^i \left(\mathcal{Z}_{k|k}^{\text{MAP},i} \right)^2 - \left(\sum_{i=1}^N \omega_k^i \mathcal{Z}_{k|k}^{\text{MAP},i} \right)^2$$

The measure $\mathcal{Z}_k^{\text{MAP}*}$ that minimizes the distance criterion under assumption of a set threshold S is used to correct the state estimation.

$$\mathcal{Z}_k^{\text{MAP}*} = \arg \min_{\mathcal{Z}^{\text{MAP}}} [d_{1m}, d_{2m}] \leq S \quad (15)$$

After the indication of the measurement $\mathcal{Z}_k^{\text{MAP}*}$, Then, it is used with the partial GPS measures and the odometer measures in order to correct the weight of th particles ω_k^i . Assuming that the measurement noise is independent, the posterior density function (16):

$$P(\mathcal{Z}_k | X_k^i) = P(\mathcal{Z}_k^{\text{PGPS}}, \mathcal{Z}_k^{\text{ODO}}, \mathcal{Z}_k^{\text{MAP}*} | X_k^i) \quad (16)$$

The log-likelihood function is:

$$V(\mathcal{Z}_k | X_k^i) \sim \|\mathcal{Z}_k^{\text{ODO}} - h^{\text{ODO}}(X_k^i)\|_{R^{\text{ODO}}}^2 + \|\mathcal{Z}_k^{\text{PGPS}} - h^{\text{PGPS}}(X_k^i)\|_{R^{\text{PGPS}}}^2 + \|\mathcal{Z}_k^{\text{MAP}*} - h^{\text{MAP}}(X_k^i)\|_{R^{\text{MAP}}}^2 \quad (17)$$

c. Total GPS outage

During total GPS outage (no pseudo-distance available) the filter fuses only the odometer and road map measures to estimate the vehicle's location. In this case the posterior density becomes (18).

$$P(\mathcal{Z}_k | X_k^i) = P(\mathcal{Z}_k^{\text{ODO}}, \mathcal{Z}_k^{\text{MAP}*} | X_k^i) \quad (18)$$

The log-likelihood function becomes:

$$V(\mathcal{Z}_k | X_k^i) \sim \|\mathcal{Z}_k^{\text{ODO}} - h^{\text{ODO}}(X_k^i)\|_{R^{\text{ODO}}}^2 + \|\mathcal{Z}_k^{\text{MAP}*} - h^{\text{MAP}}(X_k^i)\|_{R^{\text{MAP}}}^2$$

3.3. Estimation

This step involves combining the particles selected in the resampling step using a weighted sum to obtain a state estimate. Particles with high weights contribute more to the final state estimate than particles with low weights. Therefore, the resulting estimate of the state vector is given by (19).

$$\hat{X}_{k|k} = \sum_{i=1}^N \omega_k^i X_k^i \quad (19)$$

3.4. Resampling

To avoid the degeneracy problem, a resampling procedure is added to the particle filter, so that the particles with high weights are duplicated and the lowest weighted particles are deleted. There are multiple varieties of resampling algorithms to perform this step, and the performance of the particle filter can be also affected by the algorithm used. In our method, we use multinomial resampling to duplicate each particle and the rest of the particles are randomly sampled using a uniform law [0; 1] and comparing them to the cumulative sum of the weights. To avoid the weight degeneracy the number of effective particles N_{eff} is less than a set threshold N_{thresh} . The criteria used to estimate N_{eff} is given by (20).

$$N_{\text{eff}} = \frac{1}{\sum_{i=1}^N (\omega_k^i)^2} < N_{\text{thresh}} \quad (20)$$

After the multinomial resampling step, the weights are normalized, and the new weight is given by $\omega_k^i = \frac{1}{N}$.

Finally, the proposed multi-sensor fusion algorithm is presented in Figure 2. If the GPS measure is available the filter uses it only to estimate the vehicle characteristics else the filter uses the available pseudo-range data and fuses it with the odometer measures and a road map database to provide continuous localization.

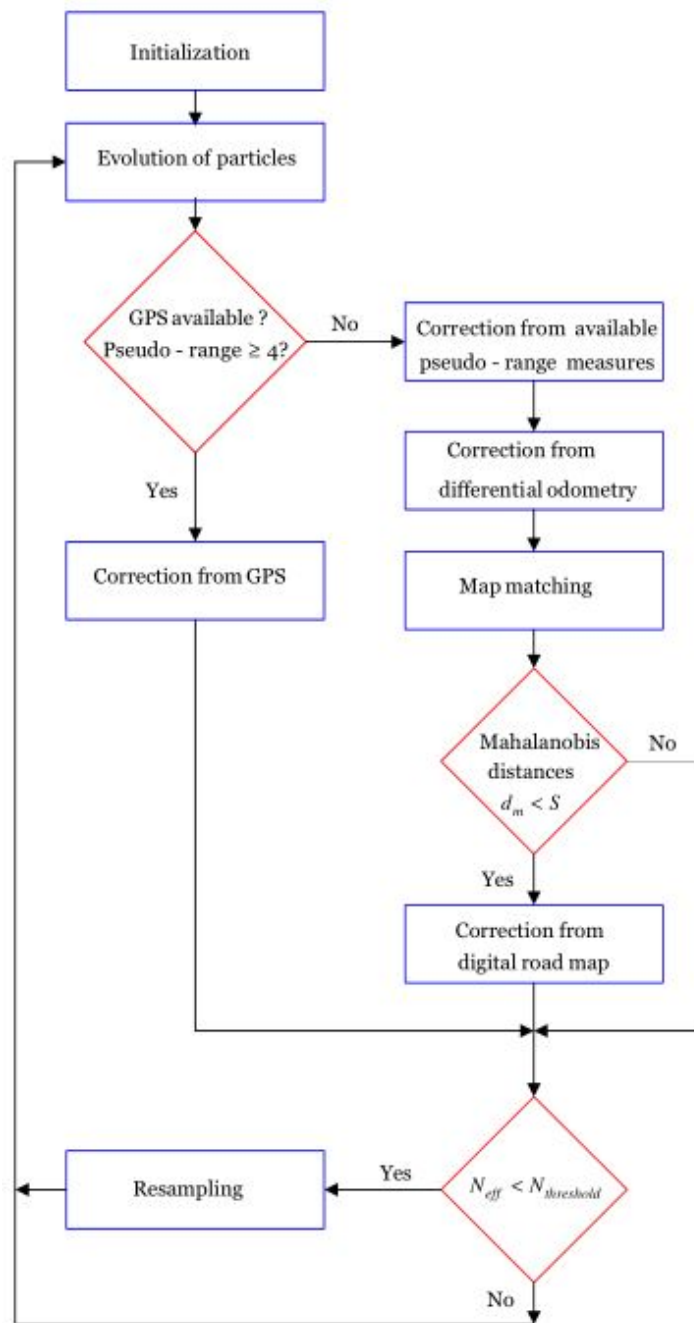


Figure 2. Localization algorithm

4. EXPERIMENTAL RESULTS

We present in this section some experimental results in order to quantify the benefits of the proposed method. We compare also these results to an EKF-based estimation. For the experimental data set, the vehicle was driven in an urban area in Calais in France. The experimental vehicle is equipped with a Novatel GPS receiver which computes the 3-D localization in the WGS84 system with a frequency of 1Hz. The speed of the vehicle is modified by many accelerations/decelerations due to the traffic lights and pedestrians. The trajectory lasts about 323 seconds with two GPS outage periods: the first one lasts 38 seconds during which the vehicle is turning right and another one of 31 seconds which the vehicle is driven in a straight line as shown in Figure 3.

In these cases, the filter fuses the available GPS pseudo-range measure (always computed from three satellites) with odometer data. The filter also exploits road map information which is delivered at a sampling rate of 1 Hz, as well as the GPS positioning when available. Note that in this work the road map is discretized into a 5 meter grid.

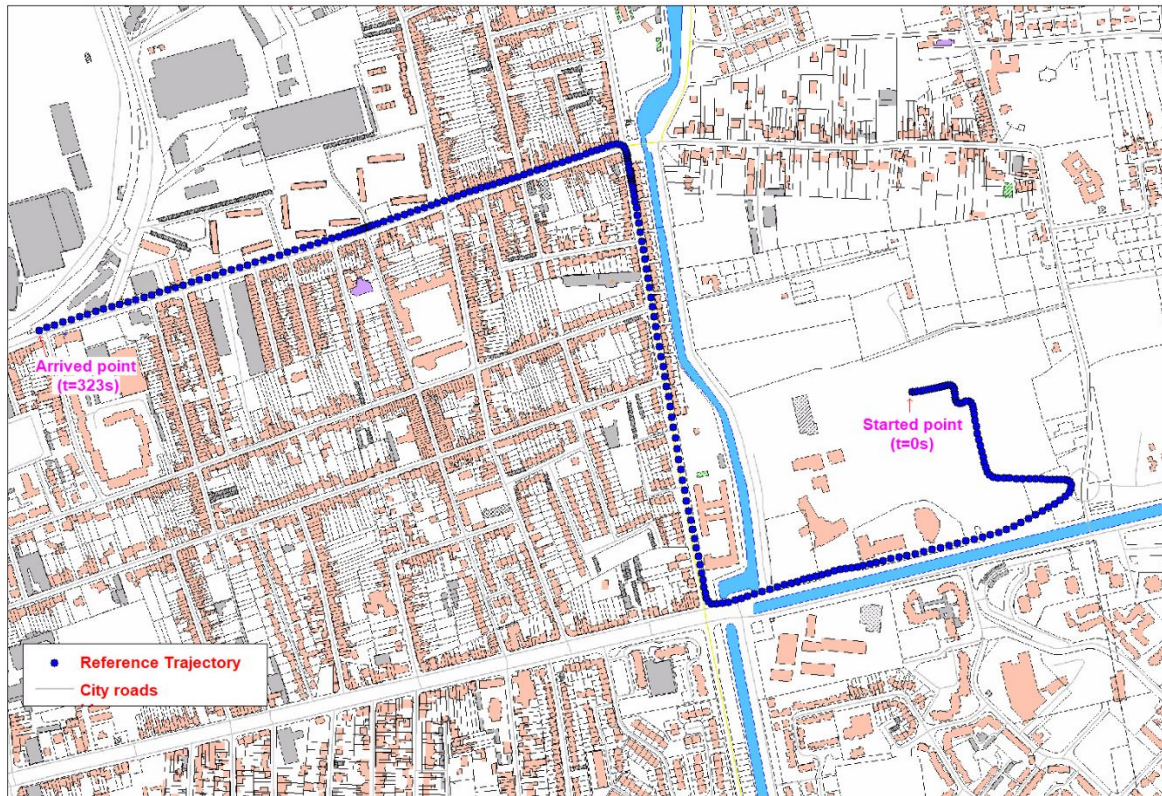


Figure 3. Reference trajectory of the vehicle

In this experimentation the covariance matrix of the GPS measurement noise is $R^{\text{GPS}} = [10 \ 0 \ 0; 0 \ 10 \ 0; 0 \ 0 \ 10]$, therefore, the associated standard deviations are $\sigma_x^{\text{GPS}} = \sigma_y^{\text{GPS}} = \sigma_z^{\text{GPS}} = 3.162 \text{ m}$. The tropospheric and ionospheric errors that affect GPS accuracy has been estimated using the Klobuchar and the Goad and Goodman model, respectively [1], [33]. For the particle filter, the covariance matrix of the odometer and map measurement noise are respectively $R^{\text{ODO}} = [0.395 \ 0 \ 0; 0 \ 0.395 \ 0; 0 \ 0 \ 0.01 \text{ rad}]$ and $R^{\text{MAP}} = [25 \text{ m} \ 0 \ 0; 0 \ 25 \text{ m} \ 0; 0 \ 0 \ 0.01 \text{ rad}]$. The used particles number is set to $N = 40.000$ and the chosen resampling threshold N_{thresh} is set to $\frac{2N}{3}$.

4.1. Vehicle motion estimation

In this section, we present the results of the proposed estimator applied to experimental data. We focus our attention on the periods of partial GPS masking. In this case, the filter uses the available partial data from the GPS, the odometric measures, and the digital road map database to estimate the trajectory of the vehicle. To evaluate the performance of our algorithm, we need to calculate the error along the travel. It has been computed using actual data, gathered by the DGPS sensor.

Figures 4 and 5 show respectively the three-dimensional acceleration and velocity errors of the vehicle. It is compared to the EKF approach that is plotted in the blue curve. We can remark that the particle filter approaches better bound the kinematics errors than the EKF when the odometers, the partial GPS measure, and the digital road map are jointly used. This plot shows also that means speed and acceleration error of PF are respectively about 1, 26 meter/second and 0,71 meter/second² when the GPS fails.

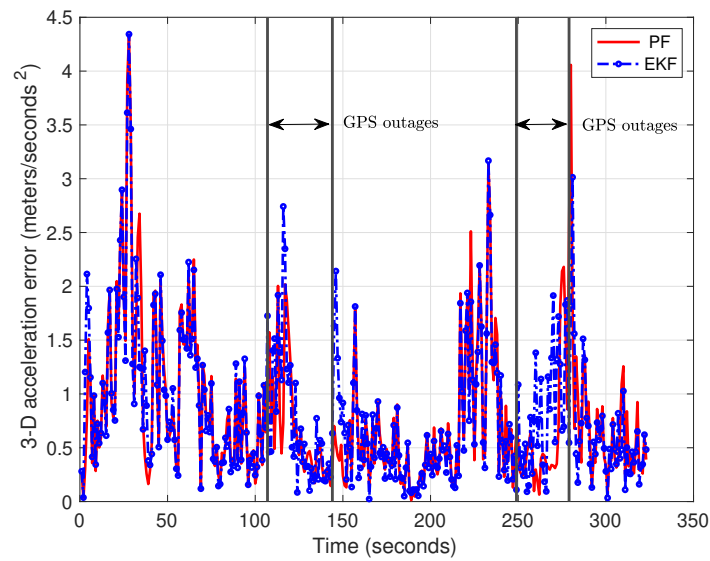


Figure 4. Plot of the 3-D acceleration error of the vehicle (PF and EKF)

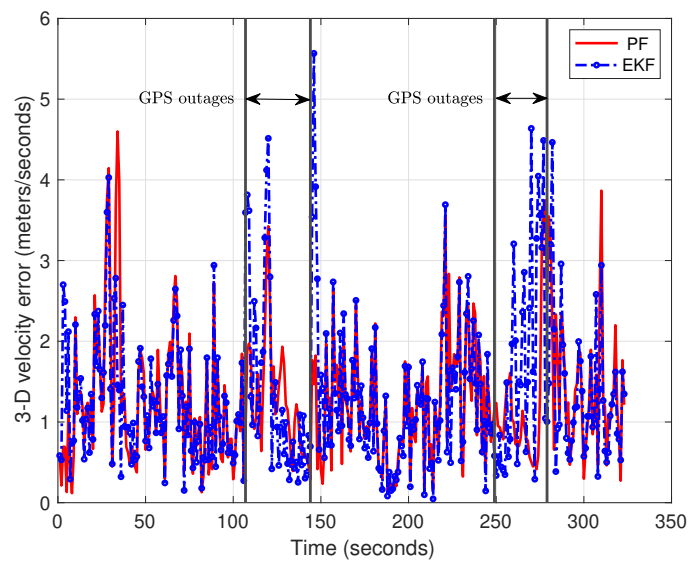


Figure 5. Plot of the 3-D speed error of the vehicle (PF and EKF)

4.2. Vehicle positioning estimation

Figure 6 shows the three-dimensional localization error of the vehicle along the travel. There are two areas where GPS positioning is absent due to an insufficient number of satellites. The first partial GPS outage lasts for 38 seconds from $t = 107$ to $t = 144$ and the second partial GPS outage lasts for 31 seconds from $t = 244$ to $t = 279$. During these periods, the mean positioning error of the particle filter method is approximately 3.23 meter. Note that the particle filter leads to better estimations accuracies in the 3-D localization, even if GPS fails.

Figure 7 shows maps of the test travel, the road polylines are plotted with the UTM coordinates (East, North) in light grey. In this figure, the PF and EKF estimated trajectory of the land vehicle are respectively plotted in green and red stars. We can remark that the proposed method improves significantly the vehicle positioning accuracy during GPS fails.

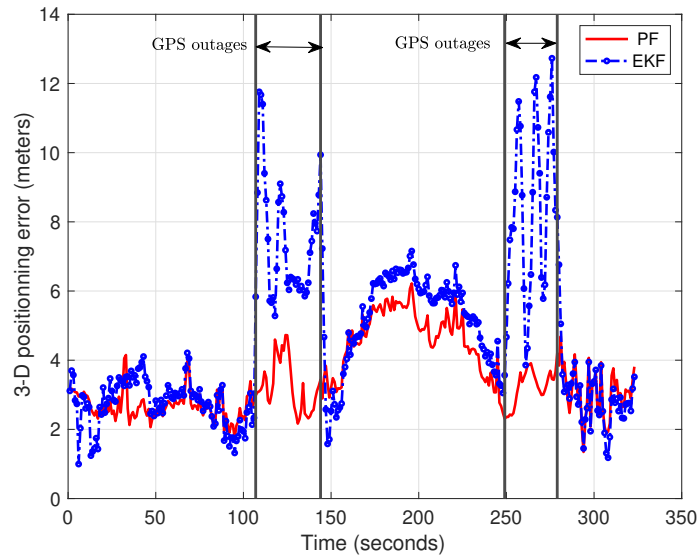


Figure 6. Plot of the 3-D localization error of the vehicle (PF and EKF)

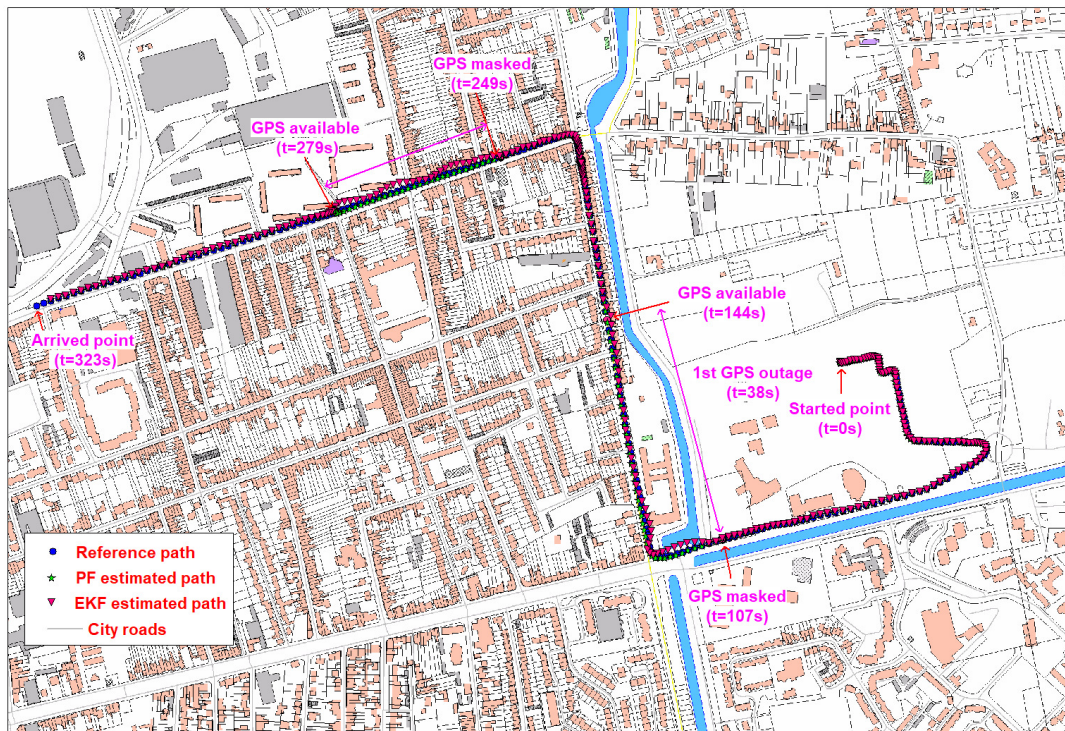


Figure 7. Reference and estimated trajectories of the vehicle

To illustrate the performance of our approach, it will be compared with the standard EKF. During the GPS outages, the reconstructed partial GPS measures (computed from the available pseudo-range), odometer sensor, and a road map database are only used for the estimated trajectory of the vehicle. The standard deviations and mean of the positioning errors during the GPS outages are presented in Tables 1 and 2 respectively. These results show that the proposed filter leads to better estimation of vehicle positioning when the GPS cannot provide a location for long time.

Table 1. Standard deviations during GPS outages

GPS Outages	$\Delta t_1 = 38$ s		$\Delta t_2 = 31$ s	
	PF	EKF	PF	EKF
3-D Acceleration (m/s ²)	0.52	0.62	0.56	0.65
3-D Velocity (m/s)	0.70	1.18	0.87	1.32
3-D Positioning (m)	0.73	2.13	0.52	2.59

Table 2. Mean error during GPS outages

GPS Outages	$\Delta t_1 = 38$ s		$\Delta t_2 = 31$ s	
	PF	EKF	PF	EKF
3-D Acceleration (m/s ²)	0.71	0.76	0.65	0.80
3-D Velocity (m/s)	1.26	1.40	1.22	1.73
3-D Positioning (m)	3.23	7.09	3.24	8.25

Figure 8 shows the evolution of the Mahalanobis distances which is our map-matching criterion here. The chosen map-matching threshold is drawn in bleu, corresponding to $S = 3$, which defines in which conditions the digital road map data can be used to improve the vehicle location. Note that the map-matching rate reaches about 92.11% for the first GPS outage and 90.31% for the second one.

Figure 9 shows the satellite availability and geometry along the travel. The satellite geometry can be quantified here using the notion of dilution of precision (GDOP), which is defined as one of the performance criteria of GPS measure. During the GPS masking, the GPS location and the GDOP value, cannot be calculated. This figure also explains that the not-perfect three-dimensional GPS localization estimation from $t = 150$ to $t = 228$ is due to the worst quality of estimated GDOP (i.e. GDOP is higher).

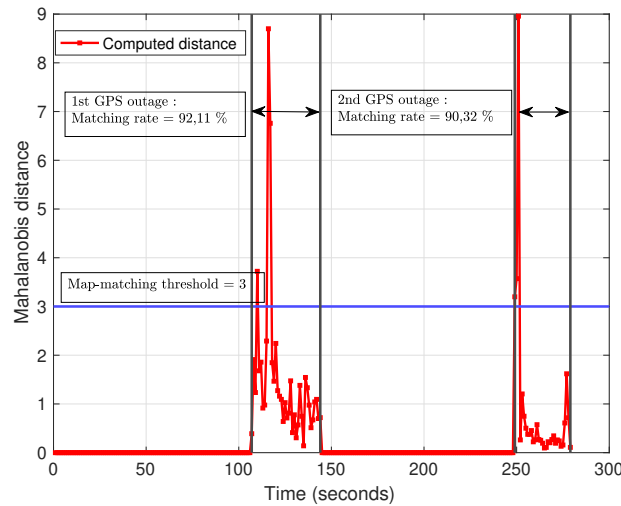


Figure 8. Time evolution of the map-matching criterion

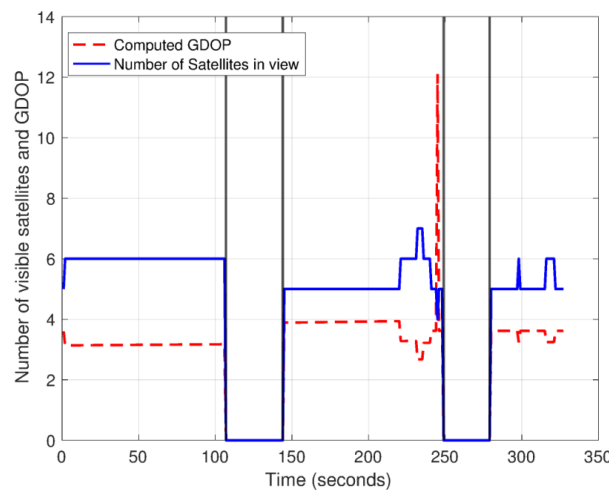


Figure 9. Time evolution of the GDOP and number of satellites in view

Finally, Figure 10 shows the road network of Calais city that we used in our experiment. The gray segments are the available road section and the one in color blue show the map measures used by our estimator using the UTM coordinates, these measurements are used to correct the estimated vehicle location. It shows also that we have 92.11% of the data were matched correctly to their concerned road sections for the first GPS outage and 90.33% for the second one. Finally, the proposed method achieves better vehicle position estimation accuracy than an EKF-based method, especially during GPS masking.

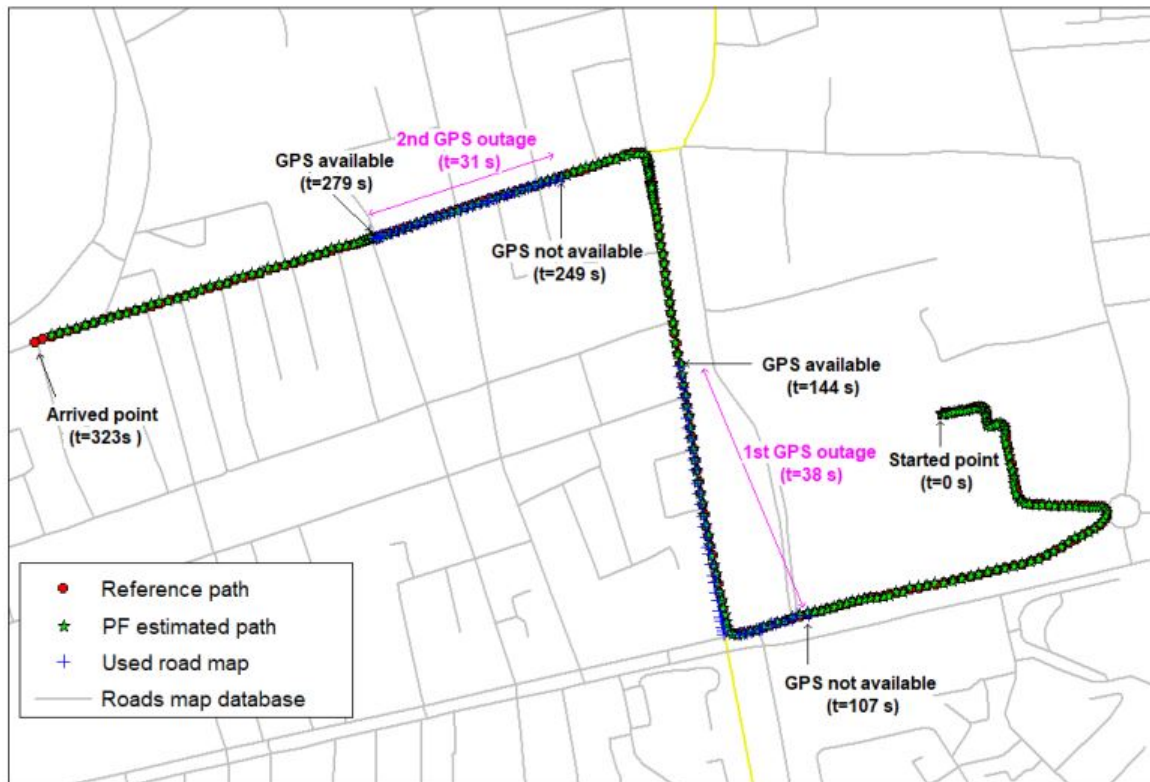


Figure 10. Estimated path of the vehicle and roadmap data positions

5. CONCLUSION

This paper presents a general method of land vehicle positioning using GPS, differential odometry, and digital road map information, especially in urban areas where the blockage of GPS satellite signals is very often. Furthermore, if the GPS measure is available and coherent (i.e. good GDOP value) the particle filter estimates the location of the vehicle using only this GPS data. Else, when the GPS fails, the available pseudo-range data, the odometer information, and the road map database, are sequentially used to estimate efficiently the vehicle pose. This estimation problem is solved by a particle filter which provides an optimal resolution scheme compared to EKF. The benefits are shown in an urban network scenario carried out in Calais, France, which demonstrates the stability and robustness of the proposed method compared to conventional EKF filters. The results show also an improvement in vehicle positioning accuracy in dense urban environments where GPS failures can occur. The proposed method can be used in several fields to provide accurate positioning. Among these fields, we can list aided positioning systems, intelligent transport systems, commercial transportation systems, and vehicle fleet management where the location information must be known accurately and at any time.

ACKNOWLEDGEMENT

The authors would like to thank professors Christophe Boucher and Jean Charle Noyer (University, Calais, France) for providing the experimental data.

REFERENCES

- [1] E. D. Kaplan and C. Hegarty, *Understanding GPS principles and applications*. Artech House, 2005.
- [2] L. Zhao, W. Y. Ochieng, M. A. Quddus, and R. B. Noland, "An extended Kalman filter algorithm for integrating GPS and low cost dead reckoning system data for vehicle performance and emissions monitoring," *Journal of Navigation*, vol. 56, no. 2, pp. 257–275, May 2003, doi: 10.1017/S0373463303002212.
- [3] Y. Zhao, *Vehicle location and navigation systems*. Artech House, 1997.
- [4] M. A. Quddus, W. Y. Ochieng, L. Zhao, and R. B. Noland, "A general map matching algorithm for transport telematics applications," *GPS Solutions*, vol. 7, no. 3, pp. 157–167, Dec. 2003, doi: 10.1007/s10291-003-0069-z.
- [5] G. Taylor, G. Blewitt, D. Steup, S. Corbett, and A. Car, "Road reduction filtering for GPS-GIS navigation," *Transactions in GIS*, vol. 5, no. 3, pp. 193–207, Jun. 2001, doi: 10.1111/1467-9671.00077.
- [6] M. Winter and G. Taylor, "Modular neural networks for map-matched GPS positioning," in *Fourth International Conference on Web Information Systems Engineering Workshops*, 2003. Proceedings., pp. 106–111, doi: 10.1109/WISEW.2003.1286792.
- [7] C. E. White, D. Bernstein, and A. L. Kornhauser, "Some map matching algorithms for personal navigation assistants," *Transportation Research Part C: Emerging Technologies*, vol. 8, no. 1–6, pp. 91–108, Feb. 2000, doi: 10.1016/S0968-090X(00)00026-7.
- [8] M. A. Quddus, W. Y. Ochieng, and R. B. Noland, "Current map-matching algorithms for transport applications: state-of-the-art and future research directions," *Transportation Research Part C: Emerging Technologies*, vol. 15, no. 5, pp. 312–328, Oct. 2007, doi: 10.1016/j.trc.2007.05.002.
- [9] R. Yozevitch and B. Ben Moshe, "A robust shadow matching algorithm for GNSS positioning," *Navigation*, vol. 62, no. 2, pp. 95–109, Sep. 2015, doi: 10.1002/navi.85.
- [10] R. Sadli, M. Afkir, A. Hadid, A. Rivencq, and A. Taleb-Ahmed, "Map-matching-based localization using camera and low-cost GPS for lane-level accuracy," *Sensors*, vol. 22, no. 7, Mar. 2022, doi: 10.3390/s22072434.
- [11] T. Song, Y. Chen, X. Li, Z. Li, and L. Xing, "A fusion map matching method for low-cost ground autonomous positioning system," *IEEE Sensors Journal*, vol. 22, no. 12, pp. 12079–12085, Jun. 2022, doi: 10.1109/JSEN.2022.3174053.
- [12] B. Gao, G. Hu, S. Gao, Y. Zhong, and C. Gu, "Multi-sensor optimal data fusion based on the adaptive fading unscented Kalman filter," *Sensors*, vol. 18, no. 2, p. 488, Feb. 2018, doi: 10.3390/s18020488.
- [13] A. Zhang, S. Bao, F. Gao, and W. Bi, "A novel strong tracking cubature Kalman filter and its application in maneuvering target tracking," *Chinese Journal of Aeronautics*, vol. 32, no. 11, pp. 2489–2502, Nov. 2019, doi: 10.1016/j.cja.2019.07.025.
- [14] S. N. Qasem, A. Ahmadian, A. Mohammadzadeh, S. Rathinasamy, and B. Pahlevanzadeh, "A type-3 logic fuzzy system: optimized by a coreentropy based Kalman filter with adaptive fuzzy kernel size," *Information Sciences*, vol. 572, pp. 424–443, Sep. 2021, doi: 10.1016/j.ins.2021.05.031.
- [15] M. F. M. Jusof *et al.*, "A Kalman-filter-based sine-cosine algorithm," in *2018 IEEE International Conference on Automatic Control and Intelligent Systems (I2CACIS)*, Oct. 2018, pp. 137–141, doi: 10.1109/I2CACIS.2018.8603711.
- [16] S. J. Julier and J. K. Uhlmann, "Unscented filtering and nonlinear estimation," in *Proceedings of the IEEE*, Mar. 2004, vol. 92, no. 3, pp. 401–422, doi: 10.1109/JPROC.2003.823141.
- [17] M. Valipour and L. A. Ricardez-Sandoval, "Abridged Gaussian sum extended Kalman filter for nonlinear state estimation under non-Gaussian process uncertainties," *Computers and Chemical Engineering*, vol. 155, Dec. 2021, doi: 10.1016/j.compchemeng.2021.107534.
- [18] F. Gustafsson *et al.*, "Particle filters for positioning, navigation, and tracking," *IEEE Transactions on Signal Processing*, vol. 50, no. 2, pp. 425–437, 2002, doi: 10.1109/78.978396.
- [19] M. S. Arulampalam, S. Maskell, N. Gordon, and T. Clapp, "A tutorial on particle filters for online nonlinear/non-Gaussian Bayesian tracking," *IEEE Transactions on Signal Processing*, vol. 50, no. 2, pp. 174–188, 2002, doi: 10.1109/78.978374.
- [20] G. Hu, W. Wang, Y. Zhong, B. Gao, and C. Gu, "A new direct filtering approach to INS/GNSS integration," *Aerospace Science and Technology*, vol. 77, pp. 755–764, Jun. 2018, doi: 10.1016/j.ast.2018.03.040.
- [21] X. Meng, H. Wang, and B. Liu, "A robust vehicle localization approach based on GNSS/IMU/DMM/LIDAR sensor fusion for autonomous vehicles," *Sensors*, vol. 17, no. 9, Sep. 2017, doi: 10.3390/s17092140.
- [22] L. Li, M. Yang, H. Li, C. Wang, and B. Wang, "Robust localization for intelligent vehicles based on compressed road scene map in urban environments," *IEEE Transactions on Intelligent Vehicles*, pp. 1–1, 2022, doi: 10.1109/TIV.2022.3162845.
- [23] A. Doucet, N. Freitas, and N. Gordon, Eds., *Sequential Monte Carlo methods in practice*. New York, NY: Springer New York, 2001.
- [24] F. Gustafsson *et al.*, "Particle filters for positioning, navigation, and tracking," *IEEE Transactions on Signal Processing*, vol. 50, no. 2, pp. 425–437, 2002, doi: 10.1109/78.978396.
- [25] E. Abbott and D. Powell, "Land-vehicle navigation using GPS," in *Proceedings of the IEEE*, 1999, vol. 87, no. 1, pp. 145–162, doi: 10.1109/5.736347.
- [26] C. Boucher, A. Lahrech, and J.-C. Noyer, "Non-linear filtering for land vehicle navigation with GPS outage," in *2004 IEEE International Conference on Systems, Man and Cybernetics (IEEE Cat. No.04CH37583)*, vol. 2, pp. 1321–1325, doi: 10.1109/ICSMC.2004.1399808.
- [27] C. Boucher, A. Lahrech, and J.-C. Noyer, "Multisensor unscented filtering for GPS-based navigation systems," in *2007 IEEE Instrumentation and Measurement Technology Conference*, May 2007, pp. 1–6, doi: 10.1109/IMTC.2007.379130.
- [28] Y. Bar-Shalom and X. R. Li, *Multitarget multisensor tracking: principles and techniques*. YBS Publication, 1995.
- [29] K. El Mokhtari, S. Reboul, J. Choquel, G. Stienne, B. Amami, and M. Benjelloun, "Circular particle fusion filter applied to map matching," *IET Intelligent Transport Systems*, vol. 11, no. 8, pp. 491–500, Oct. 2017, doi: 10.1049/iet-its.2016.0231.
- [30] M. E. El Najjar and P. Bonnifait, "A roadmap matching method for precise vehicle localization using belief theory and Kalman filtering," in *Proceedings of ICAR03 - The 11th International Conference on Advanced Robotics*, 2003, vol. 19, no. 2, pp. 1677–1682.
- [31] K. Fukunaga and L. Hostetler, "Optimization of k nearest neighbor density estimates," *IEEE Transactions on Information Theory*, vol. 19, no. 3, pp. 320–326, May 1973, doi: 10.1109/TIT.1973.1055003.
- [32] "Reprint of: Mahalanobis, P.C. (1936) 'On the generalised distance in statistics,'" *Sankhya A*, vol. 80, no. S1, pp. 1–7, 2018, doi: 10.1007/s13171-019-00164-5.
- [33] J. A. Klobuchar, "Ionospheric time-delay algorithm for single-frequency GPS users," *IEEE Transactions on Aerospace and Electronic Systems*, vol. AES-23, no. 3, pp. 325–331, 1987, doi: 10.1109/TAES.1987.310829.

BIOGRAPHIES OF AUTHORS

Abdelkabar Lahrech    obtained a Ph.D. thesis in signal processing, automatic and computer science engineering in 2006, at the Laboratoire d'Analyse des Systèmes du Littoral, Université du Littoral Côte d'Opale. Since 2009, he works as assistant professor at the faculté polydisciplinaire de khouribga, Sultan Moulay Slimane University, Morocco. His research interests include non-linear filtering, sequential Monte-Carlo methods, and multisensor fusion applied to intelligent transportation systems. He can be contacted at a.lahrech@usms.ma.



Aziz Soulhi    is a professor at the National Superior School of Rabat in Morocco. He is a doctor at the University of Lille in France. His area of research is the intelligence applied to production systems and logistics systems. He is currently president of the international congress in management and systems engineering and director of the international journal of management and systems engineering. He can be contacted at soulhi@enim.ac.ma.